Springer

Journal of Mechanical Science and Technology 23 (2009) 2521~2528

Journal of Mechanical Science and Technology

www.springerlink.com/content/1738-494x
DOI 10.1007/s12206-009-0702-z

Nonlinear behavior of micro bubbles under ultrasound due to heat transfer †

Chansoo Lim[1], Jeong Eun Kim[2], Jae Young Lee[2] and Ho-Young Kwak[1,*]

[1]*Mechanical Engineering Department, Chung-Ang University, Seoul 156-756, Korea*
[2]*Mechanical Engineering Department, Han Dong University, Pohang ,Korea*

(Manuscript Received May 6, 2008; Revised October 1, 2008; Accepted May 11, 2009)

Abstract

We investigated the nonlinear behavior of a microbubble under ultrasound, taking into account the heat transfer inside the bubble and through the bubble wall. The polytropic relation, which has been used for the process of pressure change depending on the volume variation of ideal gases, cannot properly treat heat transfer involving the oscillating bubble under ultrasound. In this study, a set of solutions of the Navier-Stokes equations for the gas inside the bubble along with an analytical treatment of the Navier-Stokes equations for the liquid adjacent to the bubble wall was used to treat properly the heat transfer process for the oscillating bubble under ultrasound. Entropy generation due to finite heat transfer, which induces the lost work during bubble evolution, reduces the collapsing process and considerably affects the nonlinear behavior of the bubble.

Keywords: Micro bubble; Heat transfer; Nonlinear behavior; Ultrasound

1. Introduction

It is well known that a cavitating bubble in liquid under ultrasound oscillates with a variety of motions according to the size of its equilibrium radius and the driving frequency and amplitude of the ultrasound [1, 2]. Usually the behavior of the bubbles under ultrasound has been investigated by the well known Rayleigh-Plesset equation with a polytropic relation for the gas inside the bubble [3]. In fact, the polytropic approximation has been widely used for the gas undergoing quasi-equilibrium process in which there is heat transfer [4]. However, the bubble behavior, which has been estimated by the Rayleigh-Plesset equation with a polytropic pressure-volume relationship, fails to account for the thermal damping effect due to heat transfer through the bubble wall, because $P_b dV$ is perfect differential [5].

Very recently, it has been observed that a sonoluminescing xenon bubble with an equilibrium radius of 15 μm in sulfuric acid solution exhibits a two-state bubble motion: the maximum bubble radius and subsequent bouncing motion varies every other cycle with alternate light emission [6]. Such an interesting nonlinear phenomenon, which cannot be observed for the sonoluminescing bubble whose equilibrium radius is about 4-6 μm in water [7], will be treated by analyzing the heat transfer inside the gas bubble and through the bubble wall. Certainly, these nonlinear phenomena of bubble motion cannot be explained by the Rayleigh-Plesset equation with the polytropic approximation because it cannot properly treat the heat transfer affecting bubble evolution under ultrasound.

2. Rayleigh-plesset equation and the energetics of the bubble motion

Considering the energy dissipation at the surface

† This paper was recommended for publication in revised form by Associate Editor Man-Yeong Ha
*Corresponding author. Tel.: +82 2 820 5278, Fax.: +82 2 826 7464
E-mail address: kwakhy@cau.ac.kr

due to viscous effects and the work done against the surface tension σ, the kinetic energy of the pulsating bubble, can be written as [8]

$$\frac{1}{2}\mathrm{M}_{\mathrm{eff}}\dot{R}_b^2 = \int_{R_0}^{R_b}\left(P_b - \frac{2\sigma}{R} - \frac{4\mu\dot{R}}{R} - P_\infty\right)4\pi R^2 dR \quad (1)$$

The effective mass "felt" by the bubble is given by the following equation:

$$\mathrm{M}_{\mathrm{eff}} = 4\pi\rho_\infty R_b^3 \quad (2)$$

The kinetic energy of the bubble with this effective mass turns out to be equal to the total kinetic energy stored in the liquid outside the bubble wall, given by

$$KE = \frac{\rho_\infty}{2}\int_{R_b}^{\infty} u^2 4\pi R^2 dR \quad (3)$$

The velocity profile in the liquid outside the bubble wall can be obtained from the continuity equation, given by $u = R_b\dot{R}_b / r^2$. Differentiating Eq. (1) with respect to R and dividing by $4\pi R_b^2\rho_\infty$, we have the well known Rayleigh-Plesset equation such as [3, 8]

$$R_b\ddot{R}_b + \frac{3}{2}\dot{R}_b^2 = \left(P_b - \frac{2\sigma}{R} - \frac{4\mu\dot{R}}{R} - P_\infty\right)/\rho_\infty \quad (4)$$

Investigating the bubble motion with the Rayleigh-Plesset equation, the gas behavior inside the bubble should be treated properly. Usually the polytropic behavior of a perfect gas [3] has been employed to obtain the gas pressure inside a uniformly compressed bubble, as in (5):

$$P_b = P_{b0}\left(\frac{R_0}{R_b}\right)^{3n} \quad (5)$$

The Rayleigh-Plesset equation with the polytropic relation, Eq. (4), may determine the bubble behavior in liquid under ultrasound. For calculation of the temperature, the following relation with variable polytropic indexes of n, related to the thermal diffusivity of gas and liquid and driving sound frequency [9], may be employed.

$$\frac{T_b}{T_\infty} = \left(\frac{R_0}{R_b}\right)^{3(n-1)} \quad (6)$$

For an air bubble under ultrasound frequency of kHz range, the polytropic index needed to calculate the temperature is about 1.3. Note that the uniform temperature obtained from Eq. (6) is valid when thermal equilibrium prevails inside the bubble. The assumption of uniform temperature is valid when the characteristic time of bubble evolution is in ms range [10].

With the polytropic relation given in Eq. (5), the instantaneous potential energy of the pulsating bubble under ultrasound can be obtained explicitly:

$$PE = \int_{R_0}^{R_b}\left(P_b - P_\infty\right)4\pi R^2 dR = \frac{4\pi}{3(1-n)}\left(P_b R_b^3 - P_\infty R_0^3\right) - \frac{4\pi P_\infty}{3}\left(R_b^3 - R_0^3\right) \quad (7)$$

where the last term indicates the consumed energy for the expansion of the bubble against the hydrostatic pressure, P_∞. Even though the above potential energy vanishes over a cycle (so that the thermal damping effect due to finite heat transfer through the bubble wall cannot be taken into account), the fictitious heat transfer rate may be obtained with the polytropic relation:

$$\frac{dQ}{dt} = \left(\frac{n-\gamma}{\gamma-1}\right)P_b \cdot 4\pi R_b^2\frac{dR_b}{dt} \quad (8)$$

3. Theory for bubble evolution under ultrasound

3.1 A set of solutions of the Navier-Stokes equations for the gas inside the bubble

The hydrodynamics related to bubble behavior in liquid under ultrasound involves solving the Navier-Stokes equations for the gas inside a bubble and the liquid adjacent to the bubble wall. The mass and momentum equations for the gas inside the bubble with spherical symmetry are given as

$$\frac{\partial\rho_g}{\partial t} + \frac{1}{r^2}\frac{\partial}{\partial r}\left(\rho_g u_g r^2\right) = 0 \quad (9)$$

$$\frac{\partial}{\partial t}\left(\rho_g u_g\right) + \frac{1}{r^2}\frac{\partial}{\partial r}\left(\rho_g u_g^2 r^2\right) + \frac{\partial P_b}{\partial r} = 0 \quad (10)$$

A set of analytical solutions for the above conservation equations [11, 12] is given as

$$\rho_g = \rho_0 + \rho_r \tag{11}$$

$$u_g = \frac{\dot{R}_b}{R_b} r \tag{12}$$

$$P_b = P_{b0} - \frac{1}{2}\left(\rho_0 + \frac{1}{2}\rho_r \right)\frac{\ddot{R}_b}{R_b} r^2 \tag{13}$$

where $\rho_0 R_b^3 = const.$ and $\rho_r = ar^2 / R_b^5$. The constant a is related to the gas mass inside a bubble by $a/m = 5(1\text{-}N_{bc})/4\pi$ with $N_{bc} = \left(P_{b0}R_b^3/T_{b0}\right)/\left(P_\infty R_0^3/T_\infty\right)$. The linear velocity profile showing the spatial inhomogeneities inside the bubble is a crucial ansatz for the homologous motion of a spherical object, which is interestingly encountered in another energy focusing mechanism of gravitational collapse [13]. The quadratic pressure profile given in Eq. (13) was verified recently by comparison with direct numerical simulations [14].

Assuming that the internal energy for the gas inside a bubble is a function of gas temperature only as $de = C_{v,b} dT_b$, the energy equation for the gas inside the bubble may be written as

$$\rho_g C_{v,b} \frac{DT_b}{Dt} = -\frac{P_b}{r^2}\frac{d}{dr}\left(r^2 u_g \right) - \frac{1}{r^2}\frac{d}{dr}\left(r^2 q_r \right) \tag{14a}$$

The viscous dissipation term in the internal energy equation also vanishes because of the linear velocity profile. Since the solutions given in Eqs. (11), (12) and (13) also satisfy the kinetic energy equation, only the internal energy equation given in Eq. (14a) needs to be solved. On the other hand, Prosperetti et al. [5] solved the internal energy equation combined with the mass and momentum equation numerically to consider heat transport inside the bubble using a simple assumption. However, heat transfer through the liquid layer, which is very important in obtaining the temperature at the bubble wall, was not considered in their study.

Using the definition of enthalpy, the internal energy equation for the gas can also be written as

$$\rho_g C_{P,b} \frac{DT_b}{Dt} = \frac{DP_b}{Dt} - \frac{1}{r^2}\frac{\partial}{\partial r}\left(r^2 q_r\right) \tag{14b}$$

Eliminating $D/Dt = \left(\partial/\partial t + u_g \partial/\partial r\right)T_b$ from Eqs. (14a) and (14b), one can obtain the following heat flow rate equation for the gas pressure inside the bubble [11, 12]:

$$\frac{DP_b}{Dt} = -\frac{\gamma P_b}{r^2}\frac{\partial}{\partial r}\left(r^2 u_g\right) - \frac{(\gamma-1)}{r^2}\frac{\partial}{\partial r}\left(r^2 q_r\right). \tag{15}$$

With the uniform pressure approximation, which is legitimate when the bubble wall acceleration is considerably less than 10^{12} m/s^2 [15], Eq. (15) can be rewritten using Eqs. (11), (12) and (13)

$$\frac{(\gamma-1)}{r^2}\frac{d}{dr}\left(r^2 q_0\right) = -\left[\frac{dP_{b0}}{dt} + 3\gamma P_{b0}\frac{\dot{R}_b}{R_b}\right] \tag{16}$$

A temperature profile can be obtained by solving Eq. (16) with the Fourier law [11]:

$$T_b(r) = \frac{B}{A}\cdot\left[-1 + \sqrt{(1+\frac{A}{B}T_{b0})^2 - 2\eta\frac{A}{B}(T_{bl} - T_\infty)(\frac{r}{R_b})^2} \right] \tag{17}$$

where A and B are the coefficients for temperature-dependent gas conductivity in these forms: $k_g = AT + B$ and $\eta = \left(R_b^3/\delta\right)/k_l/B$. For xenon, we used A = 1.031×10^{-5} J/msK^2 and B=3.916×10^{-3} J/msK [16]. The temperature distribution is given in Eq. (17) and is valid until the characteristic time of bubble evolution is of the order of the relaxation time for vibrational motion of the molecules [9] and/or is much less than the relaxation time of the translational motion of the molecules [17].

The temperature distribution due to nonuniformity of the pressure distribution, which induces an abrupt increase and subsequent decrease in the bubble wall acceleration near the collapse point, was neglected in this study because the bubble wall acceleration is considerably less than 10^{12} m/s^2. Note that no additional equation of state is needed to obtain gas pressure inside the bubble in our formulation. The detailed derivation and rationale for arriving at the temperature distribution inside the rapidly oscillating bubble are given by Kwak *et al.* [10], Kwak and Yang [11] and Kwak and Na [12].

3.2 Governing equations obtained from the Navier-Stokes equation for the liquid adjacent to the bubble wall

The mass and momentum equation for the liquid adjacent bubble wall provides the well-known equation of motion for the bubble wall [18], which is valid until the bubble wall velocity reaches the speed of sound of the liquid:

$$R_b\left(1-\frac{U_b}{C_b}\right)\frac{dU_b}{dt}+\frac{3}{2}U_b^2\left(1-\frac{U_b}{3C_b}\right)$$
$$=\frac{1}{\rho_\infty}\left(1+\frac{U_b}{C_b}+\frac{R_b}{C_b}\frac{d}{dt}\right)\left[P_B-P_s\left(t+\frac{R_b}{C_b}\right)-P_\infty\right] \quad (18)$$

The liquid pressure on the external side of the bubble wall P_B is related to the pressure inside the bubble wall P_B according to:

$$P_B=P_b-\frac{2\sigma}{R_b}-4\mu\frac{U_b}{R_b} \quad (19)$$

The driving pressure of the sound field P_s may be represented by a sinusoidal function such as $P_s=-P_A\sin\omega t$ where $\omega=2\pi f_d$.

The temperature distribution in the liquid layer adjacent to the bubble wall, which is important to determine the heat transfer through the bubble wall, is assumed to be quadratic [19]:

$$\frac{T-T_\infty}{T_{bl}-T_\infty}=\left(1-\xi\right)^2 \quad (20)$$

where $\xi=\left(r-R_b\right)/\delta$. Such a second order curve satisfies the following boundary conditions:

$$T(R_b,t)=T_{bl},\ \ T(R_b+\delta,t)=T_\infty \ \text{ and } \left(\frac{\partial T}{\partial r}\right)_{r=R_b+\delta}=0 \quad (21)$$

The mass and energy equation for the liquid layer adjacent to the bubble wall with the temperature distribution given in Eq. (20) provides a time dependent first order equation for the thermal boundary layer thickness [11]. It is given by

$$\left[1+\frac{\delta}{R_b}+\frac{3}{10}\left(\frac{\delta}{R_b}\right)^2\right]\frac{d\delta}{dt}=\frac{6\alpha}{\delta}-\left[2\frac{\delta}{R_b}+\frac{1}{2}\left(\frac{\delta}{R_b}\right)^2\right]\frac{dR_b}{dt}$$
$$-\delta\left[1+\frac{1}{2}\frac{\delta}{R_b}+\frac{1}{10}\left(\frac{\delta}{R_b}\right)^2\right]\frac{1}{T_{bl}-T_\infty}\frac{dT_{bl}}{dt} \quad (22)$$

The above equation, which was discussed in detail by Kwak and Yang [11], determines the heat flow rate through the bubble wall. The instantaneous bubble radius, bubble wall velocity and acceleration, and thermal boundary thickness obtained from Eqs. (18) and (22) provide the density, velocity, pressure and temperature profiles for the gas inside the bubble with no further assumptions. The gas temperature and pressure at the bubble center can be obtained from the ideal gas law $\rho_0 R_b^3=const.$, one of the solutions for the continuity equation given in Eq. (9).

The entropy generation rate in this kind of oscillating bubble-liquid system, which induces lost work for bubble motion, needs to be calculated by allowing for the rate change of entropy for the gas inside the bubble and the net entropy flow out of the bubble, giving the heat exchange [10]:

$$\dot{S}_g=\frac{DS_b}{Dt}-\frac{1}{T_\infty}\frac{dQ}{dt} \quad (23)$$

4. Results and discussion

Fig. 1 shows the calculated radius-time curve along with the observed results by the light scattering method [6] for a xenon bubble with R_0=15 μm, driven by an ultrasonic field with a frequency 37.8 kHz and amplitude of 1.5 atm in aqueous sulfuric acid. The calculated radius-time curve by our theory mimics the alternating pattern of the observed results, showing two states of bubble motion. On the other hand, the Rayleigh-Plesset equation with a polytropic relation, $PV^n=const.$ where n=1.3 produces the same pattern of bubble motion, as shown in Fig. 2. The bouncing motion after the first bubble collapse appears with less amplitude compared to the case with heat transfer, as shown in Fig.1. Three states of bubble motion were also observed for the sonoluminescing xenon bubble in sulfuric acid solution [20]. A cycle with quite large maximum radius after the cycle with several smaller ones appear repeated fashion as shown in Fig. 3. The bubble radius time curve calculated by our theory is in good agreement with the observed result by light scattering method [20]. However, the Rayleigh-Plesset or Keller-Miksis equation with the polytropic relation provides the same pattern of behavior each cycle, which show two bouncing motions of less amplitude after the first collapse rather than one bouncing with large amplitude.

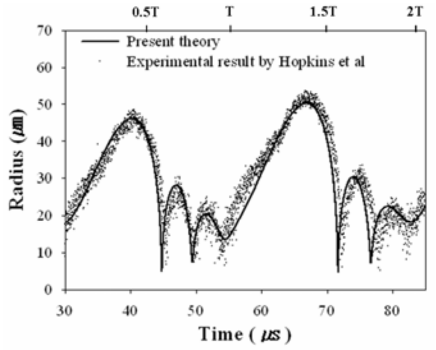

Fig. 1. Theoretical radius-time curve along with the observed one by Hopkins et al. [6] for xenon bubble of R_0=15.0 μm at P_A=1.50 atm and f_d=37.8 kHz in sulfuric acid solution. The thermodynamic properties employed for 85% sulfuric acid solution are ρ=1800 kg/m^3, C_s=1470 m/s, μ=0.025 Ns/m^2, σ=0.055 N/m, k_l=0.40 W/mK, and $C_{p,l}$=1817 J/kgK.

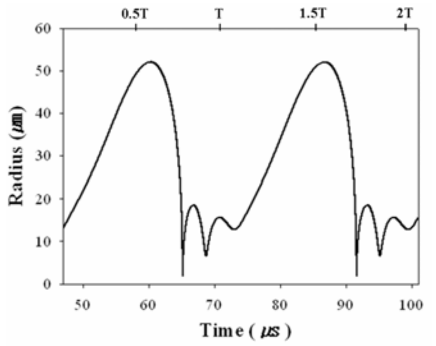

Fig. 2. Theoretical radius-time curve by the Rayleigh-Plesset equation with the polytropic assumption for the case shown in Fig. 1.

Such an outcome may be due to the heat transfer through the bubble wall, which affects the time rate change of kinetic energy around the collapse point. As can be clearly seen in Fig. 4, the amount of kinetic energy gained after the collapse is very small for the polytropic approximation. This happens because considerable kinetic energy is transferred to the liquid during the collapse phase. On the other hand, one-third of the maximum kinetic energy is regained after the first bubble collapse (in our case) where heat transfer is considered. In the insert of Fig. 4, the temporal change of the potential energy calculated by Eq. (7) is given. The potential energy may be considered as the energy transferred to the bubble by the driving ultrasound.

As is well known, the polytropic relation of $P_bV^n = const.$ is often used to model the expansion and compression of ideal gases when heat transfer

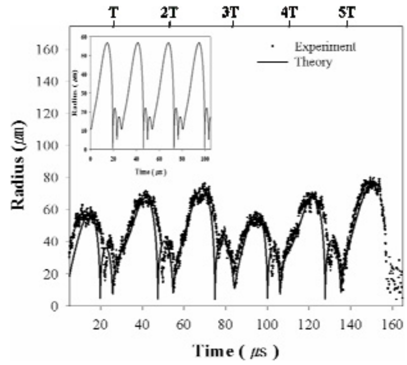

Fig. 3. Theoretical radius-time curve along with the observed results by Jeon *et al*. [20] for a xenon bubble in sulfuric acid solution. Theoretical parameter fitted to the observed result is an equilibrium radius of 14 μm under an ultrasound frequency of 37.4 kHz and an amplitude of 1.7 atm. In the insert, the bubble radius-time curve is calculated by the polytropic relation with the same equilibrium.

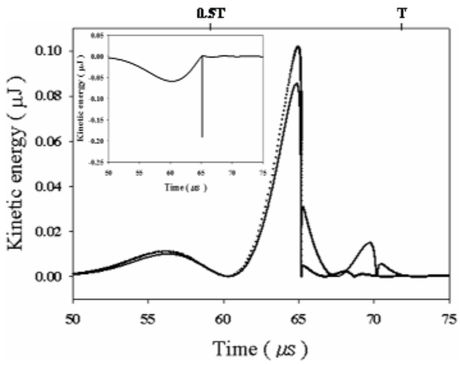

Fig. 4. Temporal change of kinetic energy calculated by our theory (——) and the polytropic relation (- - -) for the bubble shown in Fig.1. In the insert, the temporal change of the potential energy by the polytropic relation is given.

effects are present [4]. Furthermore, the polytropic relation should be used in the case of uniform temperature distribution for the gas medium where thermal equilibrium is obtained. However, a considerable temperature gradient is developed for the gas inside the bubble at the collapse point. In turn, it induces a large heat flux inside the bubble, as shown in Fig. 5. In fact, a molecular dynamic simulation for the collapsing process [21] of the bubble shown in Fig.1 produces similar magnitude of the bubble wall velocity, and the peak pressure and temperature at the collapse point as the observed [6] and theoretical results [22] when one considers the heat transfer inside the bubble and at the bubble wall.

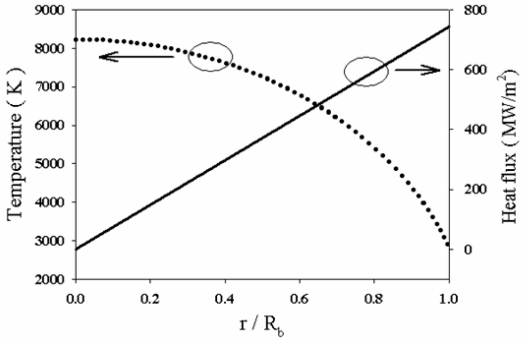

Fig. 5. Temperature distribution and heat flow rate per unit volume inside the bubble at the collapse point for the bubble shown in Fig. 1.

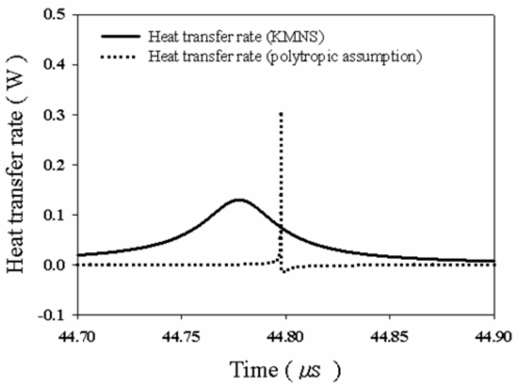

Fig. 6. Temporal heat transfer rate calculated by our theory and the Rayleigh-Plesset equation with a polytropic relation for the case shown in Fig. 1.

Fig. 6 shows the heat transfer rate as it escapes through the bubble wall into the surrounding liquid. The lost work generated during the collapse phase is just overlapped by the heat transfer rate in this particular case. The fictitious heat transfer rate calculated by Eq. (8) is also given in Fig. 6, which shows the sudden release of heat from the bubble. Such a heat transfer process is quite different from the real one. This is why the peak temperature at the collapse point, about 2800 K by the polytropic relation, is much lower than the one obtained by our theory, 6800 K, which is in close agreement with the observed result [6], as can be seen in Fig. 5.

5. Conclusion

The conventional assumption using the polytropic relation for the volume change when heat transfer effects are present proves inadequate for describing nonlinear behavior of a microbubble under ultrasound. The lost work due to finite heat transfer accompanying entropy generation should be considered for the study of nonlinear evolution of a microbubble. In this study, a set of solutions of the Navier-Stokes equations was used for the gas inside the bubble, considering heat transfer through the bubble wall and allowing for the lost work generated during bubble evolution. This, in turn, affects the temporal change of the kinetic energy of the bubble, and also, the nonlinear dynamic behavior of the bubble.

Acknowledgments

This work was supported by the Chung-Ang University Excellent Researcher Grant in 2009 and a grant from the Electric Power Research Institute (EPRI) in the U.S.A., under contract EP-P19394/C9578. Chansoo Lim has been supported by the second stage of the BK21 program and Jeong-Eun Kim has been supported by the Nuri Program.

Nomenclature

C_b : Sound speed at bubble wall
$C_{p,b}$: Heat capacity of gas at constant pressure
$C_{v,b}$: Heat capacity of gas at constant volume
e : Internal energy per mass
f_d : Driving frequency of ultrasound
k_g : Conductivity of gas
k_l : Conductivity of liquid
n : Polytropic index
P_A : Driving ultrasound amplitude
P_b : Pressure inside bubble
P_{b0} : Pressure at the bubble center
Pe : Péclet number
P_s : Driving ultrasound pressure
q_r : Heat flux inside bubble
r : Radius from the bubble center
R_0 : Equilibrium radius of bubble
R_b : Radius of bubble
$\dot{R}_b$: Bubble wall velocity
T : Period of ultrasound
T_b : Temperature of gas inside bubble
T_{bl} : Temperature at the bubble-liquid interface
T_{b0} : Temperature at the bubble center
U_b : Bubble wall velocity
u_g : Gas velocity inside bubble
t : Time

Greek letters

α	:	Thermal diffusivity of liquid
γ	:	Specific heat ratio of gas
δ	:	Thermal boundary layer thickness
μ	:	Dynamic viscosity of liquid
ρ_g	:	Gas density inside bubble
ρ_r	:	Radially dependent gas density
ρ_0	:	Gas density at the bubble center
ρ_∞	:	Density of liquid medium
σ	:	Interfacial tension
ω	:	Angular frequency of ultrasound

Subscripts

b	:	Bubble
0	:	Center
∞	:	Ambient liquid medium

References

[1] R. G. Holt and L. A. Crum, Acoustically forced oscillations of air bubbles in water: Experimental results, *J. Acoust. Sot. Am.*, 91 (1992) 1924-1932.

[2] W. Lauterborn, Numerical investigation of nonlinear oscillation of gas bubbles in liquids, *J. Acoust. Soc. Am.*, 99 (1976) 283-293.

[3] U. Parlitz,, V. English, C. Scheffczyk and W. Lauterborn, Bifurcation structure of bubble oscillators, *J. Acoust. Soc. Am.*, .88 (1990) 1061-1077.

[4] R. E. Sonntag and G. J. Van Wylen, *Introduction to Thermodynamics: Classical and Statistical*, *3rd edition*, John Wiley & Sons, New York, USA, (1991).

[5] A. Prosperetti. L. A. Crum and K. W. Commander, K. W.,Nonlinear bubble dynamicics, *J. Acoust. Soc. Am.*, 88 (1988) 1061-1077.

[6] S. D. Hopkins, S. J. Putterman, B. A. Kappus, K. S. Suslick and C. G. Camara, Dynamics of a sonoluminescing bubble in sulfuric acid, *Phys. Rev. Lett.* .95 (2005) 254301, 1-4.

[7] D. F. Gaitan, L. A. Crum, C. C. Church and R. A. Roy, R. A. Sonoluminescence and bubble dynamics for a single, stable, cavitation bubble, *J. Acoust. Soc. Am.*, 91 (1992) 3166-3183.

[8] R. E. Apfel, *Methods of Experimental Physics, Vol.19, Ultrasonics*, Academic Press, New York, USA (1981). 373.

[9] A. Prosperetti, Thermal effects and damping mechanisms in the forced radial oscillations of gas bubbles in liquids, *J. Acoust. Soc. Am.*, 61 (1977) 17-27.

[10] H. Kwak, S. Oh and C. Park, C., Bubble dynamics on the evolving bubble formed from the droplet at the superheat limit, *Int. J. Heat Mass Transfer*, .38 (1995) 1707-1718.

[11] H. Kwak and H. Yang, An aspect of sonoluminescence from hydrodynamic theory, *J. Phys. Soc. Jap.* 64 (1995) 1980-1992.

[12] H. Kwak and J. Na, Physical processes for single bubble sonoluminescence, *J. Phys. Soc, Jap.* 66 (1997) 3074-3083.

[13] J. Jun and H. Kwak, Gravitational collapse of Newtonian stars, *Int. J. Mod. Phys. D*, .9 (2000) 35-42.

[14] H. Lin., B.D. Storey and A.J. Szeri, Inertially driven inhomogenieties in violently collapsing bubbles: the validity of the Rayleigh-Plessset equation, *J. Fluid Mech.*, 452 (2002) 145-162.

[15] H. Kwak and Na, J., Hydrodynamic solutions for a sonoluminescing gas bubble, *Phys. Rev. Lett.*, 77 (1996) 4454-4457.

[16] J. Kestin, K. Knierim, E. A. Masson, B. Najafi, S. T. Ro and M. Waldman, Equilibrium and transport properties of the noble gases and their mixtures at low density, *J. Phys. Chem. Ref. Data*, 13 (1984) 229-303.

[17] K. Byun, H. Kwak and S. Karng, Bubble evolution and radiation mechanism for laser-induced collapsing bubble in water, *Jap. J. Appl. Phys.*, 43 (2004).6364-6370.

[18] J. B. Keller and M. Miksis, Bubble oscillations of large amplitude, *J. Acoust. Soc. Am.*, 68 (1980) 628-633.

[19] T. Theofanous, L. Biasi and H. S. Isbin, A theoretical study on bubble growth in constant and time-dependant pressure fields, *Chem. Eng. Sci.*, 24 (1969) 885-897.

[20] J. Jeon, C. Lim and H. Kwak, Measurement of pulse width from sonoluminescing gas bubble in sulfuric acid solution, *J. Phys. Soc. Jpn*, 77 (2008) 033703, 1-4.

[21] K. Y. Kim, C. Lim, H. Kwak and J. H. Kim, Validation of molecular dynamic simulation for a collapsing process of sonoluminescing gas bubble, *Molecular Physics*, 106 (2008) 967-975.

[22] K. Kim, B. Byun and H. Kwak, Characteristics of sonoluminescing bubbles in aqueous solutions of sulfuric acid, *J. Phys. Soc. Jpn.*, 75 (2006) 114705, 1-7.

Chansoo Lim received B.S. and M.S. degrees in mechanical engineering from Chung-Ang University in 2007 and 2009, respectively. He has been working at Doosan Heavy Industries & Construction since his gra-duation.

Ho-Young Kwak received B.S. degree in physics from Seoul National University in 1971 and M.A. in plasma physics and Ph.D. in mechanical engineering from the University of Texas at Austin, USA in 1978 and 1981, respectively. He joined mechanical engineering faculty, Chung-Ang University , Korea in 1981 and is currently Professor there. Bubble nucleation, bubble dynamics, sonoluminescence phenomena, synthesis of specialty of nano-catalysts under multi-bubble sonoluminescence condition, electronic equipment cooling and exergetic and thermoeconomic analysis of thermal systems are of his research interest.